



Project no. TIP5-CT-2006-031415

INNOTRACK

Integrated Project (IP)

Thematic Priority 6: Sustainable Development, Global Change and Ecosystems

D4.3.7

Innovative laboratory tests for rail steels

Final report

Due date of deliverable: 2009-06-30

Actual submission date: 2009-10-05

Start date of project: 2006-09-01

Duration: 36 months

Organisation name of lead contractor for this deliverable:

Deutsche Bahn AG

Revision: final

Project co-funded by the European Commission within the Sixth Framework Programme (2002-2006)		
Dissemination Level		
PU	Public	x
PP	Restricted to other programme participants (including the Commission Services)	
RE	Restricted to a group specified by the consortium (including the Commission Services)	
CO	Confidential, only for members of the consortium (including the Commission Services)	

Table of Contents

Glossary	3
1. Executive Summary	4
2. Introduction	5
3. Overview of laboratory test capabilities	6
3.1 The SUROS Twin Disk Machine (UoN).....	6
3.2 The VAS Test Rig.....	6
3.3 Test Rig C (DB)	8
4. Test planning and test performing.....	10
4.1 Testing matrix	10
4.2 Execution of tests	10
4.3 Test results	12
4.3.1 <i>Twin disk tests</i>	12
4.3.2 <i>Full-scale tests at the VAS test rig</i>	14
4.3.3 <i>Full-scale tests at the DB rig</i>	15
4.4 Evaluation of the tests: metallographical examination, material degradation and EBSD	15
5. Numerical simulations of the laboratory tests.....	17
5.1 Comparison of contact conditions	17
5.2 RCF predictions from test rigs	18
5.2.1 <i>RCF predictions based on “engineering” models</i>	18
5.2.2 <i>Comments on RCF predictions based on “engineering” models</i>	20
5.2.3 <i>RCF predictions based on finite element (FE) simulations</i>	21
5.2.4 <i>Conclusions and recommendations</i>	22
6. Overall assessment of the tests	23
7. Conclusion.....	25
8. References.....	26
9. Appendix 1: Measurement of RCF under laboratory testing conditions	27
General	27
Surface Cracks.....	27
Subsurface Cracks.....	29

Glossary

Chalmers	Chalmers University of Technology, Gothenburg
CORUS	Corus Rail Technologies
DB	Deutsche Bahn
TUD	Technical University Delft
UoN	University of Newcastle
VAS	voestalpine Schienen GmbH
HC	Head checks
RCF	Rolling contact fatigue
SUROS Machine	<u>S</u> heffield <u>U</u> niversity <u>R</u> olling <u>S</u> liding [Twin-Disk Machine]
VAS test rig	linear test rig used by VAS for testing rail segments
DB test rig A	test rig used by DB for full-scale wheel on roller tests at high speed
DB test rig C	test rig used by DB for full-scale wheel on roller tests at heavy load

1. Executive Summary

This paper presents a first thorough investigation of different laboratory tests for rail materials combined with numerical simulations and metallographic investigations. A specific methodology for the latter is given in the Appendix.

Laboratory tests for new rail materials are desirable supplements to field tests in order to save time and money. Thus, less valuable products can be early withdrawn from expensive field tests.

Within this work package, test conditions for laboratory tests of rail materials have been defined and compared to field conditions. Existing test equipment and evaluation methods of the WP partners have been exploited for the laboratory tests in order to find out the applicability to the pre-defined field conditions.

The tests were performed at the SUROS twin disk test machine, at the VAS linear full-scale test rig and at DB full-scale roller rigs. The results were compared among other with respect to metallography and material deterioration.

Subsequent numerical calculations showed that the full-scale tests more or less deviate systematically from the expected contact conditions due to bending of wheel and rail. In addition, predictions regarding RCF have been carried out and compared to test results.

It is shown that twin disk tests as well as tests on a full-scale linear test rig are suitable for practical use. The tests on full-scale roller rigs failed due to the need for specific rail samples, which ultimately destroyed the fixtures during the tests.

An evaluation of the different tests including a rough estimate of effort is given.

2. Introduction

The activities of WP 4.3 were focussed on the reduction of cost for testing of new rail and switch material which is of practical importance for railway infrastructure operators as well as for rail industry. When new rail materials are brought into service the infrastructure operator usually tries to find the steel grade that best fits his requirements at specific locations as in curved or inclined track, at acceleration sections etc. On the other hand, steel manufacturers try to find out correlations between the chemical and metallurgic features of the material and its behaviour in the track.

Rail tests are usually being performed as field tests on specific rail sites. The reasons for additional laboratory tests within the INNOTRACK programme are

1. Although the current CEN standard on rail steels (EN13674-1) has all basic material property tests their direct relevance to in service performance remains a subject of debate, especially regarding RCF, which is one of the key rail degradation effects now. As the programme focuses on LCC reduction, laboratory tests could provide a link between metallurgy and rail-wheel contact mechanics that would affect future rail steel developments in order to reduce rail maintenance costs.
2. Controlled tests in the laboratory will enable extrapolation of the observed site results to a greater range of duty conditions.
3. The cost and time required for laboratory tests can be easily estimated and controlled.

For these purposes laboratory tests have been planned and carried out within WP 4.3. The tests used different test rigs by VAS, UoN, and DB in order to simulate RCF and wheel/rail wear under defined contact conditions. One purpose of the tests was to compare the different results tests. Numerical simulations were used in order to allow an understanding of specific features of the test rigs.

Another purpose of the tests was to connect the behaviour of the material tested to practical experience from the field. Field tests are carried out by installing rail samples into a highly frequented track. Field tests usually have a high acceptance by local managers because their results are repeatable. On the other hand, the results of field tests are strictly related to that location, need a long time, and are cost-expensive.

It was the aim of WP 4.3 to provide a set of laboratory tests for rail material, which reflect the expected performance of rail steels in service better. Another aim was to derive material features from these tests that characterizes the behaviour of the materials in situ.

The challenge was to identify material parameters that are of relevance for the rail integrity. Therefore, the link between metallurgy and rail-wheel contact mechanics needs to be mechanistically justified rather than empirically if the industry is to target future rail steel developments. In this context, it is important to examine the microstructural changes that occur due to the stresses induced by passing traffic and their association with rail grades and the presence of RCF cracks.

3. Overview of laboratory test capabilities

3.1 The SUROS Twin Disk Machine (UoN)

The SUROS twin-disk machine has been designed to simulate a wheel in rolling/sliding contact with a rail (Figure 3.1-1). The disk specimens are cut from rail and wheel sections. Usual dimensions are 47mm diameter and 10mm track (running) width. These dimensions make it possible to machine specimens from real rail and wheel sections (Figure 3.1-2).

The rail disk is driven at a fixed speed by the lathe, and the wheel disk is driven by an A/C motor; the speed of the wheel disk, and thus the relative (longitudinal) slip, can therefore be controlled precisely. During testing, an eddy-current probe is used to check for cracks.

Water or other lubricants can be applied during testing. The tests reported here were done under dry and alternating dry/wet conditions.

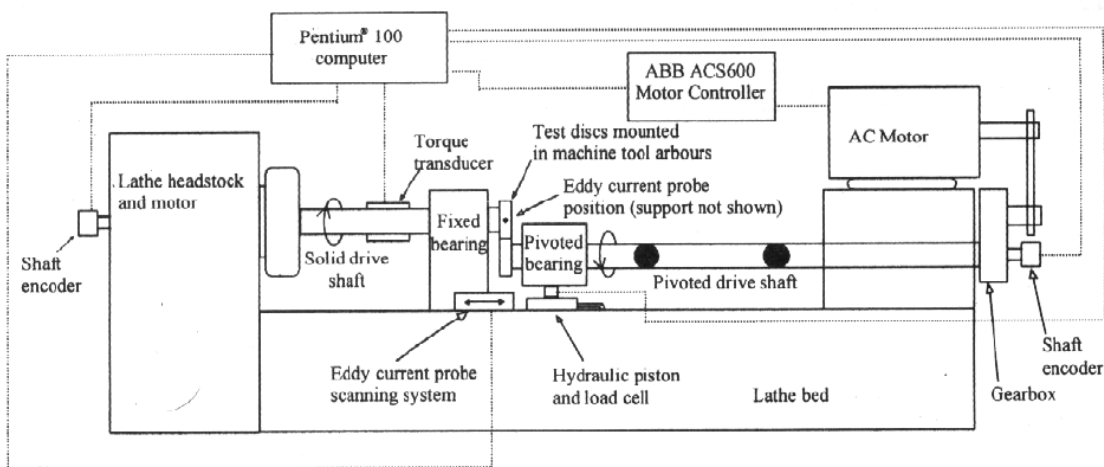


Figure 3.1-1: Schematic of SUROS twin-disk machine.

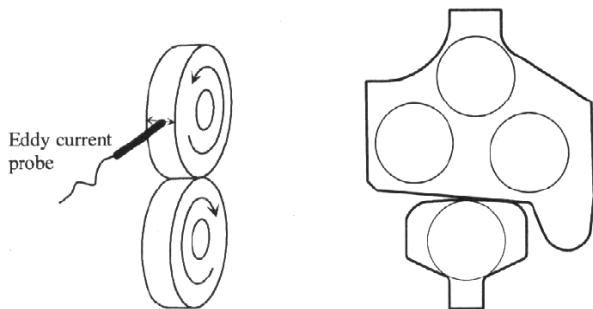


Figure 3.1-2: Disk specimens for twin disk tests at SUROS test machine.

3.2 The VAS Test Rig

The VAS test rig is a linear test stand, which consists of a 1.5m piece of test rail being attached to a carriage, which moves hydraulically underneath a common locomotive or freight wheel.

The test rig can simulate uni-directional or bi-directional traffic conditions. Here, only uni-directional running was simulated. For uni-directional running, the wheel is lifted up while the rail carriage is returning at the end of a pass, and then gently set down on the rail to start another rolling cycle.

The speed of the test rig is limited to 1m/s, allowing a maximum of 33,000 wheel passes in a 24-hour period. Forces are measured within the hydraulic cylinders. Rail and wheel positions are recorded in all three

dimensions with displacement sensors. Room temperature and air humidity are recorded during each test. All measured data is stored in a database for post processing and test evaluation.

The following loads can be applied to the wheel-rail contact (Figure 3.2-1)

- Vertical (N): up to 1.000 kN
- Lateral (Q): up to 100 kN
- Longitudinal (braking or accelerating) (T): up to 35 kN

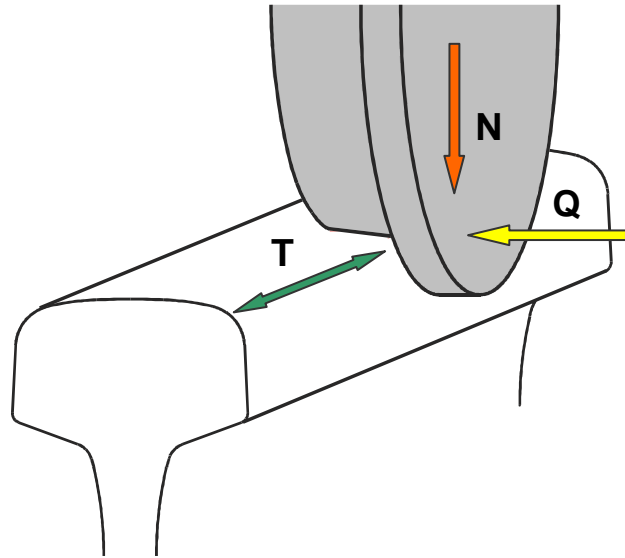


Figure 3.2-1: Loading conditions - forces

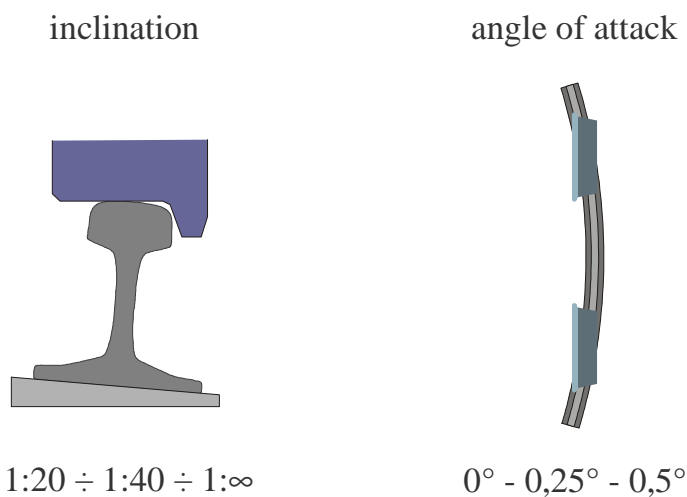


Figure 3.2-2: Contact situations on VAS test rig

The angle of attack between wheel and rail can be set either to 0, 0.25 or to 0.5 degrees allowing different curve radii to be simulated. Rail cant is adjustable with a ribbed base plate or wedge to alter wheel-rail contact conditions.

After preliminary tests with alternating wet/dry contact conditions had not delivered results of necessary stability, the subsequent tests were done under dry conditions.

3.3 Test Rig C (DB)

The test rig C of DB consists of a wheelset on the size of the original, which is driven on a pair of rail rollers with a diameter of 2100 mm. The test rig is able to apply the following loads:

- Vertical (N): up to 300 kN
- Lateral (Q): up to 100 kN
- Longitudinal (braking or accelerating) (T): none

The test rig runs at a maximum speed of about 160 km/h (100 mph). Thus, a number of about 25.000 wheel passes can be applied per hour, which would allow time-lapse tests with a time reduction of 150:1.

For the tests planned within WP 4.3 one of the roller rims was exceptionally prepared with a construction specifically designed for this purpose. It was equipped with a pair of bended railheads. The railheads were taken from a regular rail of R260 steel grade. The rail pieces were mounted closely and were fixed by collets to the inner part of the roller. The gap between them was less than 1 mm.

The test situation is shown in Figure 3.3-1.

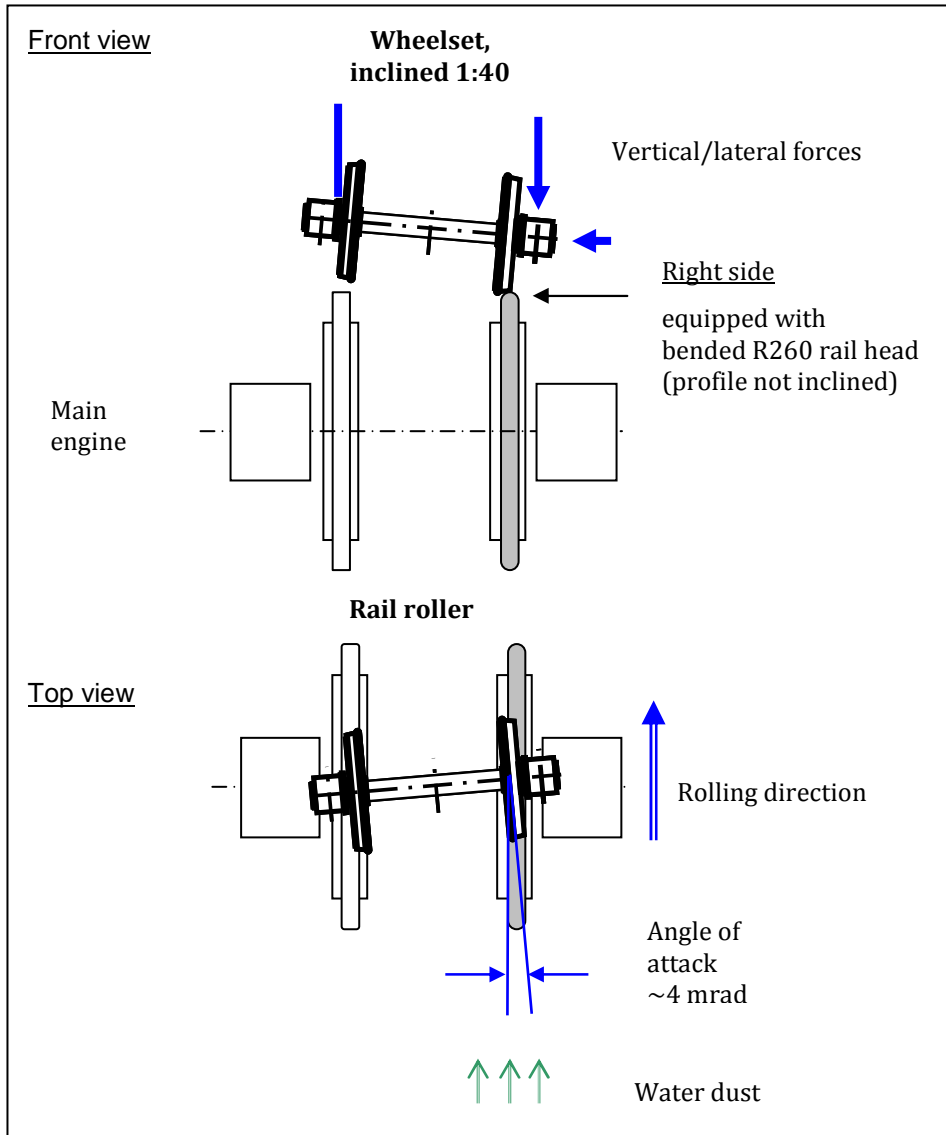


Figure 3.3-1: Test conditions at DB test rig C.

The wheel and rail got new profiles before testing. The inclination between the profiles was applied by inclining the wheelset about 1:40. Thus, only one side of the wheel came into contact. The vertical load was applied with magnitudes according to operational axle loads. An angle of attack was applied by turning the wheelset about the vertical axis against the gauge corner in the rolling direction.

A water spray driven by compressed air was applied permanently to the contact point.

Finally, the test situation described failed on test rig C when the collets fractured after a large number of load cycles. Therefore, DB provided related results from another, similar wheel/rail test rig, test rig A.

4. Test planning and test performing

4.1 Testing matrix

A testing matrix was established in order to define comparable conditions for the laboratory tests at the different rigs. For details, see [1]

The conditions refer to the operational conditions of typical passenger cars moving through a curved track. The project partners intended to define conditions that usually lead to RCF and wear at the railhead. They clarified that the experimental investigations and modelling are targeted in the area most useful for a technical stable railway operation. Therefore, it was not expected to use extreme conditions such as high speed or heavy load traffic

The contact conditions of the testing matrix at the full-scale test rigs relate to a high-speed car moving through a curve of 800 m radius or a straight track. The twin disk test rig used an equivalent normal pressure. It is the only rig, which can apply a pre-defined longitudinal slip.

Table 1: Testing matrix

	<u>1. SUROS Twin disk</u>	<u>2. VAS RSP</u>	<u>3. DB Rig C (A)</u>
A: Fixed conditions			
Rail profile/inclination	N/A	60 E2 / 1:40	60 E2 / 1:40
Wheel Profile	N/A	S1002	S1002
Wheel steel grade	R7	R7	R7
Longitudinal Slip	Controllable, 1%	Limited	none
Lubrication	Water/Dry	Water/Dry	Water
Lateral load	None	40 kN or lower	low (<10 kN)
B: Variable conditions			
Vertical load	Equivalent contact pressure	200 kN and 150 kN per wheel	80 kN per wheel
Angle of attack	0°	0°, 0.25°	0°, 0.25°
Rail steel grade	260, 350 HT, 400HB	R260 (R350 HT, 400HB)	R260, R350 HT (400 HB)

4.2 Execution of tests

The tests were performed in order to

- to demonstrate the applicability of the test conditions to the test rigs,
- to achieve first results of material tests
- to provide input data for numerical calculations.

The table below gives an overview on the tests done within WP4.3 after preliminary tests showed the applicability of the testing matrix. For the preliminary tests, see [3].

Table 2: Overview on WP 4.3 tests

Name of test	perfor- mer/ Test rig	material pairing	Forces/ Pressure/slip	test conditions Cycles dry/wet	results
INNOT-07/08 a/08 b /-09/-17/-22	UoN/ SUROS	CORUS 260 vs. R7&R8T	1500 MPa, 1% slip	5k dry/10k dry/10k wet/ 15k dry/20k wet 15k dry, vs. R8T	see [7]
INNOT-13/-14/-41 /-51/-16/-23	UoN/ SUROS	CORUS 350 vs. R7&R8T	1500 MPa, 1% slip	see above	see [7]
INNOT-01/02a/02 b /-03/-18/-24	UoN/ SUROS	CORUS 400 vs. R7&R8T	1500 MPa, 1% slip	see above	see [7]
INNOT-04/-05a/05b /-06/-21/-25	UoN/ SUROS	VA 350 vs. R7&R8T	1500 MPa, 1% slip	see above	see [7]
INNOT-10/12a/12b /-11/-19/-26	UoN/ SUROS	VA 400 vs. R7&R8T	1500 MPa, 1% slip	see above	see [7]
260-20-wet #1	VAS/ Test rig	R260 vs. R7	20t vert. / 4t lat. / free slip	100K passes wet, water supply temporarily interrupted	Wear RCF/HC after 10 – 50 k passes; see D4.3.3 [3]
260-20-wet #2	VAS/ Test rig	R260 vs. R7	20t vert. / 4t lat. / free slip	100k passes wet, continuous water supply	Wear No HC; see D4.3.3 [3]
<i>R260-20 wet #3-#6 R260-15 wet #1 Wassertest R260-0 wet #1</i>	<i>VAS/ Test rig</i>	<i>R260 vs. R7</i>	<i>preliminary tests regarding water supply and rail inclination</i>		<i>not evaluated</i>
<i>400UHC dry #1-#2 R260 dry#1 R350HT dry#1 MHH dry#1 R260 Vergleich 1- 20R260 dry#2 R260 dry N1</i>	<i>VAS/ Test rig</i>	<i>R260 vs. R7</i>	<i>consistency tests, tests discarded</i>		<i>not evaluated</i>
R260 60E2 dry	VAS/ Test rig	R260 vs. R7	20t vert. / 4t lat. / free slip	125K passes, dry	see [8]
R350HT 60E2 dry	VAS/ Test rig	R350HT vs. R7	20t vert. / 4t lat. / free slip	125K passes, dry	see [8]
400BHN 60E1 dry	VAS/ Test rig	R460BHN vs. R7	20t vert. / 4t lat. / free slip	125K passes, dry	see [8]
DB C01	DB/test rig C	R260 vs. R7	8t vert. / ~1t lat. / free slip	1,200K cycles wet (continuous)	Wear No HC, see D4.3.3 [3]
DB A01	DB/test rig A	R260 vs. R7	7t vert. / ~0,5t lat. / free slip	680K cycles mixed (1/3 wet, 2/3 dry)	Wear RCF/HC at test end, see D4.3.3 [3]

Not all test results could be finally evaluated. The main reason was that the conditions sometimes became instable, especially for the full-scale tests. Therefore, some tests had to be repeated or substituted. The reasons for the instability where:

- instable friction coefficients, i.e. a non-varying friction level could not always be ensured under laboratory conditions
- malfunction of force measurement
- mechanical malfunction, i.e. breaking of samples and clamps after very high numbers of load cycles.

4.3 Test results

4.3.1 Twin disk tests

The results obtained by UoN at the SUROS test rig are reported in a separate document [7] available at the INNTRACK KMS. Five different rail materials

- CORUS 260
- CORUS 350
- CORUS 400
- VA 350 (voestalpine)
- VA 400 (voestalpine)

were tested versus wheels of R7 and R8T steel grade provided by VAS. The tests were performed under dry and wet conditions.

Figure 4.3-1 shows material loss over a total of 5 k and 15k load cycles under dry conditions.

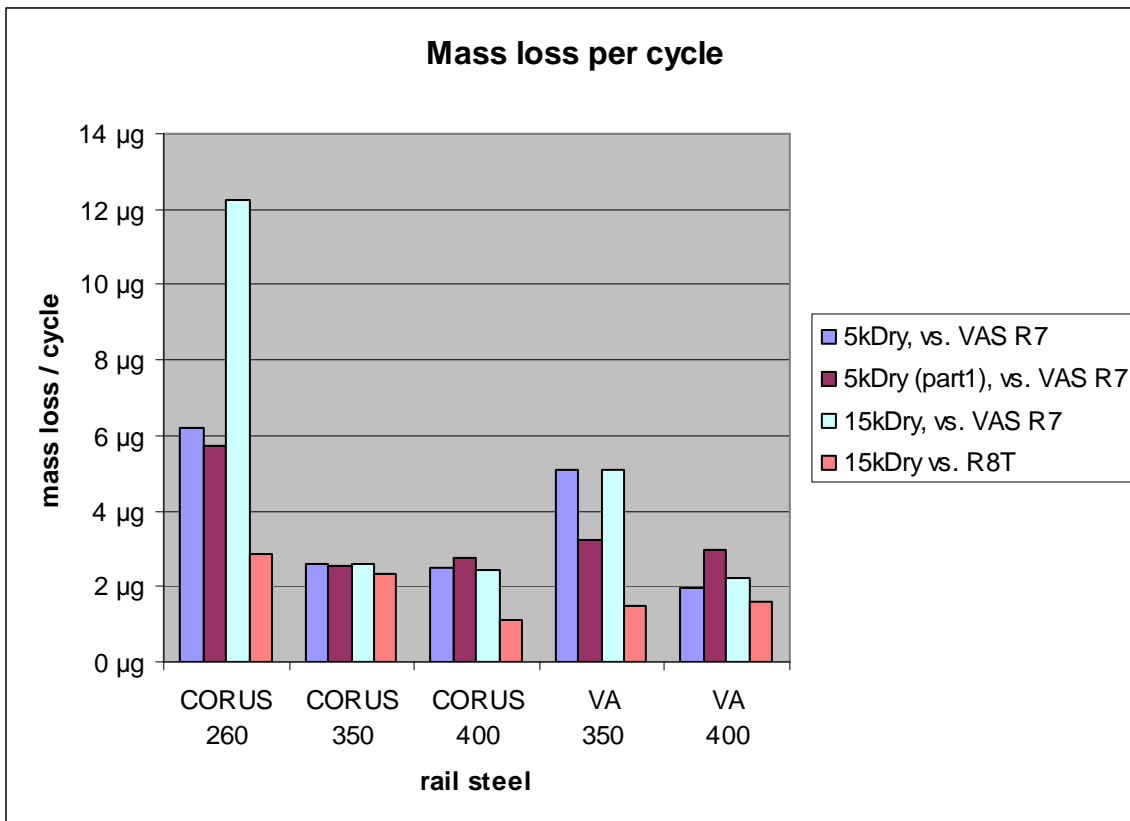


Figure 4.3-1: Twin disk tests, mass loss per cycle, dry conditions

It appears from the figure that

- (1) the wear rates of the rail material decrease when the steel hardness increases from about 260 to about 400 N/mm²,
- (2) the wear rate is nearly independent of the total number of cycles under dry conditions, and thus the results are rather stable – with the one exception of Corus 260 where an unexpected high the wear rate occurs,
- (3) the mass loss depends on the wheel steel grade too. Here, the harder wheel steel (R8T) causes a slightly lower wear of the rails.

As mentioned above, some tests were made to establish test configurations with realistic friction coefficients, i.e. with application of water. Here, the SUROS tests used two configurations for all rail steel grades:

- One test was the continuation of the dry 5k Dry cycles test (part 1) with subsequent 5k Wet cycles (part 2). I.e. the weight of the specimen was only established after 5k cycles and then the test continued with application of water.
- The second was a test under fully wet conditions during 20k cycles

The results are shown in

Figure 4.3-2.

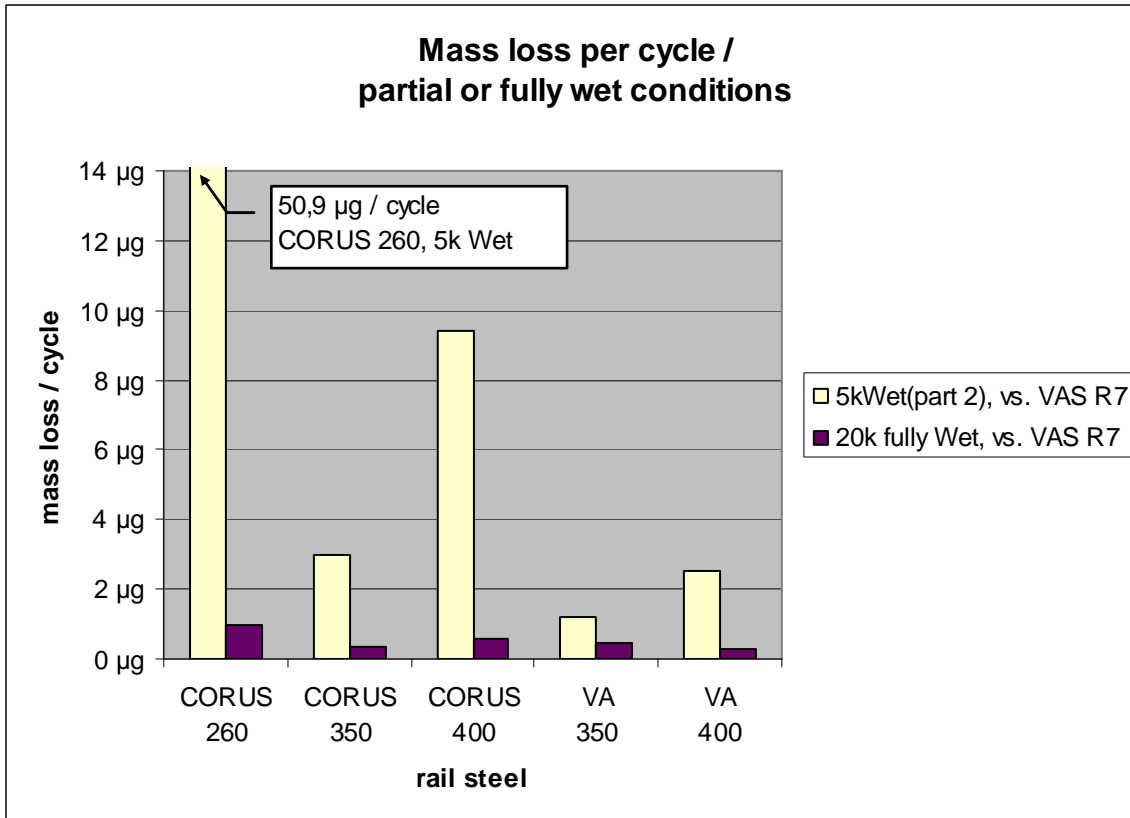


Figure 4.3-2: Twin disk tests, mass loss per cycle, wet conditions

It appears from

Figure 4.3-2 that

- (4) The 20k cycle's tests with permanent application of water shows lower wear rates than the dry tests for all rail steel grades tested. This was expected because the friction coefficient is decreased.
- (5) On the other hand, the wet tests following preceding dry wear show irregular tendencies: For the CORUS 260 grade, the wear rate is extremely high. In addition to that, the other rail steel grades do not show regular tendencies of the wear rates neither in comparison to the dry conditions nor with respect to the hardness of the rail steel.

The metallurgical analysis of the worn specimen has shown that the reason for this deviation from expectations is a more or less intense spalling at the rim of the specimen. It could be established that the wet/dry conditions produce 2-4 times more cracks per mm than the dry tests. In addition, the material depth damaged by the cracks is increased by a similar factor of 2-4. For more details, see [7].

Conclusion:

The tests demonstrate the ability of twin disk tests to evaluate wear and RCF of different rail steels. Trends such as the decrease of wear and RCF with increasing strength could be established, see

Figure 4.3-2.

The twin disk tests represent a good way of testing materials under closely controlled conditions, however, when using the laboratory results to understand real field behaviour of rail steels two points should be kept in mind. First, the twin disk conditions represent extreme cases of wear under completely dry and clean high friction conditions, or of continuous wet running. In reality, rails are rarely completely clean, and even in rain, the first wheel of the leading bogie will displace most water from the rail, and later wheels will see less water at the rail-wheel contact. Secondly, the twin disk simulation cannot be used to study the effect of rail-wheel profiles, since these are not present in the test.

The extreme and rapidly repeated conditions in twin disk testing help to reveal differences between the materials, but in translating the results to the field it should be remembered that such severe conditions are rarely encountered repeatedly over long periods. Therefore, the twin disk data should be used for input to modelling rather than direct translation to field behaviour. When the performance for each individual rail-wheel contact is known, the models can be used to combine wear and cracking predictions to different contact conditions, and give a prediction of how the steels will perform when subject to a range of contact conditions. Real performance of the rail steels will be moderated by frequent changes in conditions, and factors such as less clean rails (giving lower friction, less wear) and less rapidly repeated wet contacts (less rapid crack growth).

4.3.2 Full-scale tests at the VAS test rig

Wear results: The profile wear was first determined by W1, W2, and W3, which are defined as the profile deviations in vertical, lateral, and diagonal direction, see

Figure 4.3-3. These standard wear measurements did not show usable results as plastic flow on the rail surface often resulted in “negative wear” at these measurement points. As an alternative, the worn “area loss” in the contact zone was calculated.

The results for W1 and for the area loss can be seen in

Figure 4.3-3. Both clearly show the improved wear resistance of the steels of higher grade.

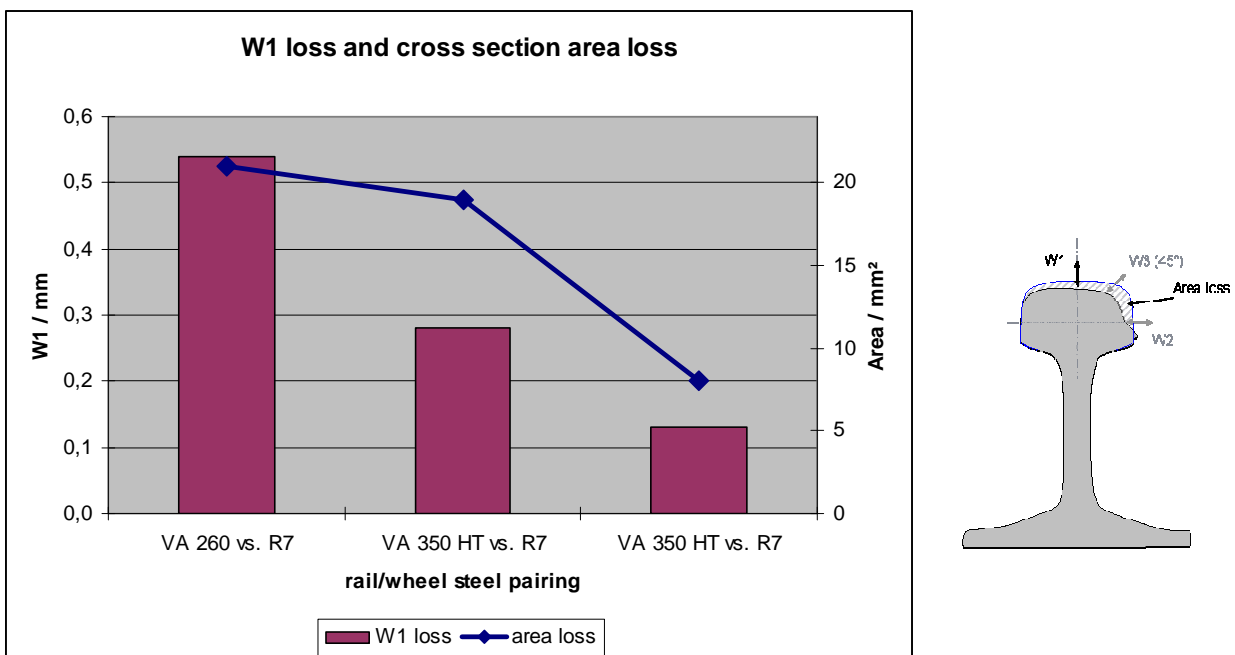


Figure 4.3-3: VAS tests: results of wear measurement

RCF results: In two preliminary tests reported in D4.3.3 it had been established that tests with water lubrication resulted in no head check formation at the VAS rig. Only tests with almost no water application led to HC formation. So it was decided to run subsequent tests completely dry.

Under dry conditions, all three rail steels formed RCF cracks. With increasing rail grade the longitudinal distance between the cracks on the surface is reduced. The 400BHN grade showed the lowest crack depths of all three grades despite having also the lowest final wear. More details, including photographs and metallographic investigations may be found in [8].

Conclusion:

The voestalpine full-scale rail-wheel test rig was able to provide evidence that an increased wear resistance comes along with an increased RCF resistance of pearlitic rail steels.

A number of differences between real track conditions and the test rig were identified:

- Only one wheel: due to the lack of an axle connected with a second wheel no steering forces will act in the wheel-rail contact.
- Closed environment: no rain, moisture, residuals, sand etc. will contaminate the wheel-rail contact resulting in an assumed high friction coefficient of 0.6 for the whole test.
- Same rail underneath same wheel: As the same wheel always gets into contact with the same piece of rail, an unusual wear adaption of the two partners takes place resulting in wear rates and wear profiles that might not be seen in track.

Although differences to real track conditions exist, the test rig of voestalpine clearly shows the same trends as seen in track: heat-treated rail grades (R350HT, 400BHN grade) show an increased wear and RCF resistance as compared to standard, i.e. non-heat-treated rail grade R260.

Because of the INNOTRACK test results voestalpine started an upgrade program for the test rig in order to provide test conditions that are even more close to real contact conditions.

4.3.3 Full-scale tests at the DB rig

RCF results: The test 'DB C01' at a roller rig with continuous water application did only produce microscopic head checks after 20 MGT or 1.2m load cycles. The cracks could be identified by metallographic examination as reported in [6].

It was not possible to repeat the tests at DB Rig C because parts of the rig as e.g. the fixing and the railhead failed under cyclic loading of the test.

By contrast, usual tests at DB's roller rig A (reported in [3] as DB A01) with intermittent application of water dust do generate HC at less than 10 MGT or 0.6m load cycles. The examination of these results was used instead of the tests failed.

Conclusion:

The attempt to establish a stable test procedure with exchangeable rail material on a roller rig has failed due to excessive requirements on the fixing of the rail. Nevertheless steady contact conditions could be established during the tests. These could be evaluated, by contact simulations and material investigations.

4.4 Evaluation of the tests: metallographical examination, material degradation and EBSD

After the tests have been performed, the test results were evaluated. The WP4.3 group decided to adopt a methodology proposed by Corus to examine and compare samples from test rigs and from rail sites, see Appendix 1.

In addition, examinations for material degradation by use of the Electron Back Scatter Diffraction (EBSD) technique were performed by Corus. This technology has been described in [2]. It was used in order to

extract material characteristics relevant to steel degradation. The task was to enable a mechanistic understanding of degradation and to extrapolate the observed results to a greater range of duty conditions.

For metallurgical demands it is important to emphasize that the link between metallurgy and rail-wheel contact mechanics needs to be mechanistic rather than empirical in order to target future rail steel developments. The characterization of wear and RCF for different rail grades provides comparative results for different rail grades and for different contact conditions.

The depth of damaged layer, characterized by material degradation, was determined for several samples from different network having different RCF status. Table 3 shows an overview for an assessment of microstructural damage of the samples taken from the track. It can be seen that the depth of damage strongly decreases with an increase of the steel grade – independent on the RCF status.

Table 3: Depth of damaged layer at network samples

Steel grade	Sample from Network	Track form	RCF Status category of the samples					Max. depth of "Damaged layer"
			Free	Light	Mo-derate	Heavy	Severe	
220	NR	ballasted	X	X	X	X	X	>5mm
260	NR	ballasted	X			X		2.5 ...3.5 mm (ballasted), <1mm in a desert railway with high abrasive wear
	Other UK	Slabtrack				X		
	Other RoW	ballasted	X					
	DB	ballasted		X	X	X	X	
350HT	NR	ballasted		X			X	2-3 mm (ballasted)
400HB+	ProRail	ballasted					X	<1mm (ballasted)

These findings were compared to findings of EBSD analysis from three test rig samples (1 from the DB test rig and 2 from Corus twin disk tests) with the following results:

- The DB rig sample reveals lower depth of damage than observed in track.
- The twin disk samples show similar behaviour to track.

Conclusion:

The overall EBSD analysis appears to be a promising technique for assessing depth of damage and is able to discriminate between rail grades.

In some cases, EBSD analysis was able to distinguish between test rig samples and operational rails.

5. Numerical simulations of the laboratory tests

It is not possible to reproduce field conditions in laboratory tests fully. This becomes obvious if it is considered that not even the field conditions at two locations along a stretch of track are identical. Thus, a representative measure is needed to translate the conditions in the laboratory to those in the field. A rough such measure is e.g., the total amount of applied loading to rolling contact fatigue (RCF) initiation. However, such a measure does not account for variables such as the contact geometry, which thus implicitly are considered identical between laboratory and field.

A more general approach would be to define an equivalent measure that can be related to the RCF life of the rail. The RCF resistance of the rail can then be estimated by comparing the evaluated magnitude of the equivalent measure for the laboratory set-up to the measured RCF life. Further, by evaluating the equivalent measure for field conditions the rail life at the studied location can be estimated from the rail's RCF resistance. In addition, the equivalent measure can be employed to compare different laboratory set-ups.

Naturally a similar approach can be (and is) adopted for quantities such as wear rates, noise emissions etc, but the current evaluation focuses on RCF.

The current discussion is based on work reported in WP4.3 deliverables D4.3.4 [4] and D4.3.5 [5]. The focus on the discussion is to highlight possibilities and difficulties with the outlined approaches.

5.1 Comparison of contact conditions

Any equivalent measure for RCF prediction needs to account for the wheel–rail contact conditions. This includes the location of the contact, the contact patch size, and the distribution and magnitude of the normal contact stresses as will be discussed in this section. It also includes the distribution and magnitude of the tangential contact stresses, which is also discussed in the next section.

In [4] a methodology for simulation of wheel-rail rolling contact and its application to laboratory tests is presented, followed by a methodology for wear calculation.

Data were taken from the laboratory tests of the three rigs with their different configuration and complexity. The measured profiles and the corresponding loading were used as inputs for simulations. The outputs were checked against measurements and observations during the tests.

The results of the comparison of contact conditions are shown in Table 4.

Table 4: Maximum shear stresses, locations, and rail inclinations calculated

	UoN SUROS	VAS WET 1	DB rig C
Max. shear stress	0.675 GPa ($\mu = 0.45$)	0.59 – 1.0 GPa ($\mu = 0.45$)	0.75 – 0.83 GPa ($\mu = 0.2$) 0.41 – 0.47 GPa ($\mu = 0.1$)
Location of max shear stress	Across the cylindrical surface	3 – 11 mm from inner rail side	Broad area, 10 – 36 mm from inner rail side
Kind of contact	line contact	1- or 2-point	1-, 2-point or multiple contact
rail inclination, designed	-	1:40	1:40
rail inclination, ascertained by simulation	-	1:172	~1:100

The results can be interpreted as follows

1. The coefficient of friction μ could only be measured at the SUROS machine giving a range of 0.4 – 0.45 for the first 5,000 dry cycles. An estimate of $\mu = 0.45$ was made for the VAS WET 1 test in accordance to the SUROS test and a range of $\mu = 0.1 \dots 0.2$ for the DB test due to its constant water application.

As appears from the table that the maximal shear stress is of the same order between 0.59 and 1.0 GPa for all test configurations with the exception of DB rig C and $\mu=0.1$.

2. The location of the maximum shear stress for the VAS rig HC is 3 – 11 mm from rail inner side, which is in good agreement with the actual measured HC location of 2 – 8 mm from the inner side of the test rail. This part of the rail was first worn into conformal contact before HC initiate.
3. For the DB rig C test, the contact is mainly on top of the rail and part of the gauge shoulder, the predicted location of the maximal stress is between 10 – 36 mm from the inner rail side, in agreement with the location of embryonic cracks. The difference in the locations of maximal stress and cracks of the VAS and DB tests reflects the difference in the test conditions. Observations indicate that RCF initiation location varies under operation conditions.
4. The effective rail inclination of the full-scale rigs differed from the design configuration. This was found to be due to deformation in the load chain of the rig.
It should be noted and considered e.g. in multi-body-simulations that the same deformation occurs in real life when rails, axles and wheels are bending under the load of the vehicle.

The above discussion may indicate that though the complexity of the rigs differs, the stress and the damage the materials experienced may be comparable under certain load and friction conditions. The extent of their comparability was further investigated by subsequent wear, metallurgical, micro-structural and fatigue analyses.

Though there was deformation in the load chain at the VAS rig, the rail profile measurements is consistent and smooth within measurement error tolerance. This indicates that the contact conditions were stable.

5.2 RCF predictions from test rigs

The prediction of RCF life sets out from the results in [4] (discussed in section 5.1 above). Two main approaches were adopted:

1. An “engineering” approach where RCF life was predicted directly from evaluated contact stresses
2. A finite element based approach

5.2.1 RCF predictions based on “engineering” models

Here “engineering” models denote models that relate the RCF life to interfacial wheel–rail contact stresses. Other approaches also include parameters such as wheel–rail slip; however, these could not be employed in this study due to reasons that will be discussed below.

In the current study two equivalent measures have been adopted

1. The maximum interfacial shear stress, τ_{\max} .
2. A RCF index based on the shakedown map, see [9] and [10]. The index can be expressed as

$$FI_{\text{surf}} = f - \frac{k}{p_0} > 0 \quad (1)$$

where f is the traction coefficient, k the yield limit in shear of the rail material (in the current study adopted as $k = 300$ MPa), and p_0 the maximum contact pressure according to hertzian theory. RCF is predicted for $FI_{\text{surf}} > 0$. Details and discussions on numerical complications are given in [4].

A key issue for both of these criteria is the magnitude of the interfacial shear. An important concept here is “full slip”, which means that the (local) interfacial friction stress τ is proportional to the contact pressure p , i.e. $\tau = \mu \cdot p$ where μ is the maximum coefficient of friction. The peak interfacial friction stress will under full slip conditions have a magnitude of $\tau_{\max} = \mu \cdot p_0$ and the traction coefficient will equal the maximum coefficient of friction, i.e. $f = \mu$.

In the analysis, τ_{max} was evaluated under the presumption of full slip for the twin disk configuration and by using non-Hertzian contact mechanics analysis for the DB and VAS test rigs. Note that these contact mechanics simulations do not account for the rolling motion between wheel and rail.

Further, in the analysis the traction coefficient f has been evaluated under the presumption of full slip. The validity of this presumption will be discussed below.

Evaluation of predictive capabilities of the criteria

The current study considers three tests featuring similar materials. The test conditions cover a wide span of operational conditions.

In order to evaluate the predictive capabilities of the criteria it is noted that for steel there is a (more or less) linear relationship between the logarithm of the applied stress amplitude versus the logarithm of the total number of cycles to failure N . This relationship is referred to as the Wöhler or S–N-curve.

If the loading is more complex (as is the case here), the common approach (which is adopted here) is to compensate by introducing an equivalent measure. The suitability of the equivalent measure can then be judged by whether a more or less linear relationship exists between the logarithm of the fatigue life and the logarithm of the equivalent measure.

Predicted magnitudes of equivalent measures $F_{l_{surf}}$ and τ_{max} are summarized in Table 5.

Table 5: Summary of RCF parameters of various criteria for the studied test conditions.

RCF criterion	Twin-disk, dry	Twin-disk, lubricated	VAS	DB
$F_{l_{surf}}$ ($k = 300$ MPa)	0.2 to 0.25	-0.05 to 0	0.09 to 0.14	0.03 to 0.08
τ_{max}	600 to 675 MPa	225 to 300 MPa	590 MPa	750 MPa
Observations during the tests	Initiated cracks and surface flakes before 5 000 cycles.	Surface flaking by 5000 cycles following the dry test stage.	Head check initiation after 20 000 to 50 000 passes.	No head check initiation after about 1.2 million cycles. Embryonic cracks found in microscopy examinations.

The RCF predictions are presented in Figure 5.2-1. Based on the discussion above, it is clear that τ_{max} is not a suitable equivalent measure, whereas $F_{l_{surf}}$ shows a very promising trend. Note that the poor performance of τ_{max} is largely a consequence of the omission of interfacial shear due to the rolling motion.

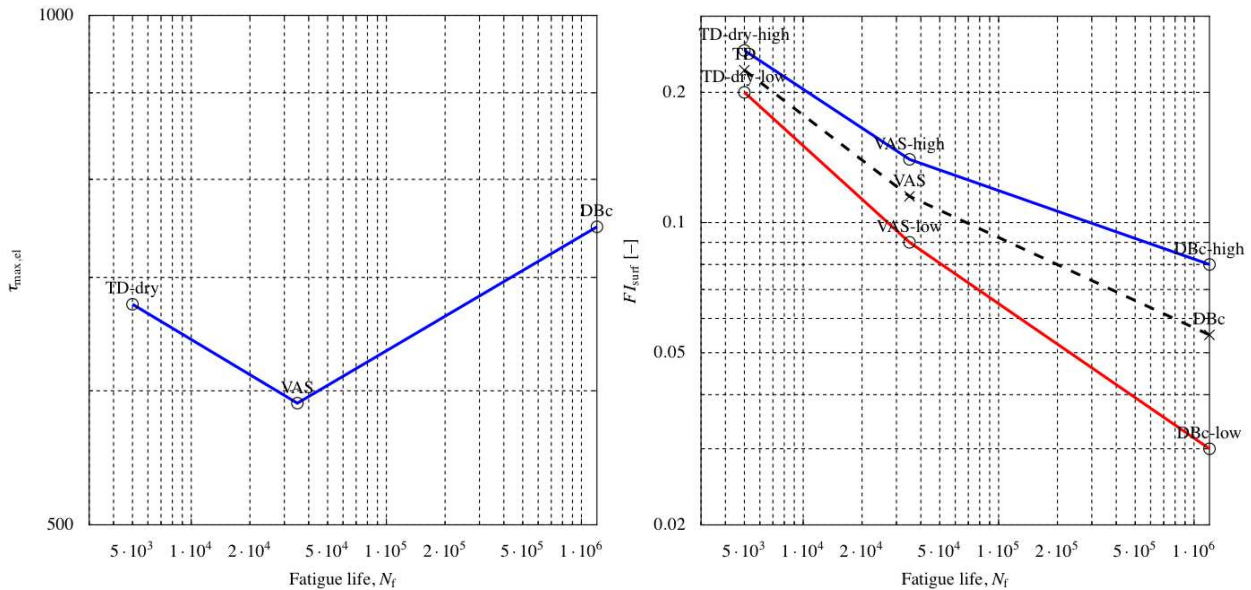


Figure 5.2-1: Log-log-plot of equivalent measures (τ_{max} and $F_{l,surf}$) versus RCF life. For $F_{l,surf}$ the upper graph corresponds to a high and the lower graph to a low estimation of the traction coefficient. The dashed line corresponds to the mean value.

5.2.2 Comments on RCF predictions based on “engineering” models

Results for twin disk tests

The set-up featured Corus 400 rail steel vs. R7 wheel steel for dry conditions giving a range of $\mu \approx 0.4$ to 0.45 followed by a wet phase with $\mu \approx 0.15$ to 0.2. The cylindrical disks have a line contact with maximum Hertzian contact pressure of 1500 MPa.

Presuming full slip the peak elastic shear stress alters between 600 to 675 MPa for the dry and 225 to 300 MPa for the lubricated cycles. If the cyclic yield limit in shear is presumed to be $k = 300$ MPa, then the fatigue index $F_{l,surf}$ is

- for the dry phase, between 0.20 and 0.25, i.e. RCF is likely or
- for the wet phase, between -0.05 and 0, i.e. RCF is improbable

The simulation results coincide with previous tests on the SUROS machine where surface flakes of stable depth develop under dry conditions, even though the surface is also wearing. The wet phase is not likely to promote any further RCF initiation. However, as is well known [9], the lubrication will promote growth of initiated cracks. Consequently, the prediction supports the observed mechanism of crack initiation during the dry phase followed by crack propagation during the wet phase. The RCF initiation life is taken as the number of dry cycles.

The presumption of full slip adopted for the evaluation of τ_{max} and f should be very valid for the studied configuration since the relative slip between the disks is controlled to promote full slip conditions.

Results for VAS full-scale tests

The traction coefficient was estimated based on the presumption of full slip. τ_{max} was evaluated from a non-Hertzian contact mechanics analysis. The contact patch size was deduced from the contact mechanics simulations detailed in [4]. It should be noted that these simulations did not account for the rolling motion.

The results of simulation for full slip conditions indicate a range for $F_{l,surf}$ between 0.09 and 0.14. This coincides to the observation that RCF occurred during the VAS tests.

The presumption of full slip is not supported by the magnitude of the directly applied lateral force. However, additional simulations of the dynamic interaction between the wheel and the rail indicate major additional tangential forces due to the rolling motion and the conformal contact. In particular, there is a large contribution to the total creep forces from the longitudinal creep, which relates to the inability of the conformal profile to steer solely by conicity. Note that the evaluation of τ_{\max} did not account for these stresses.

To get an exact magnitude of this additional tangential force proved to be very cumbersome for two reasons:

1. The numerical simulation of dynamic wheel–rail interaction cannot account for the non-hertzian contact conditions due to the conformal contact.
2. The magnitude of the tangential contact forces is extremely sensitive to the contact geometry. Even the small variation in contact geometry along the piece of rail adopted in the laboratory simulations gave a major influence.

In conclusion, the presumption of full slip cannot be fully verified, but the simulation reported in [5] makes it plausible.

Results for DB full-scale tests

The contact patch size was deduced from the contact mechanics simulations detailed in [4]. The traction coefficient was estimated based on the presumption of full slip.

The simulations for fully wet slip conditions indicate a range for $F_{I_{\text{surf}}}$ between 0.03 and 0.08. This indicates that RCF should occur, but that we are very close to the fatigue limit (presumed at $F_{I_{\text{surf}}} = 0$). Although this test configuration had the highest elastic shear stress in the quasi-static contact stress evaluation, only “embryonic” cracks were observed during the tests. The reason why no macroscopic RCF was observed could relate to a varying lateral load, which probably spreads out the fatigue damage over a wider area.

5.2.3 RCF predictions based on finite element (FE) simulations

The “engineering” models require a very limited amount of material characteristics. Since they are based on elastic theory, the elasticity modulus and Poisson’s ratio are needed. For $F_{I_{\text{sub}}}$ also, the yield limit in shear is adopted, but this is basically a normalisation parameter and could be excluded.

Another approach is to perform a more detailed evaluation of contact stresses and material deformation and translate the evaluated material response to an equivalent measure. This has been demonstrated in [5] where elasto-plastic simulations of the wheel–rail rolling contact have been carried out. These simulations include an evaluation of the contact stresses including additional interfacial shear stresses due to rolling. Further, they are more reliable in that they do not presume elastic conditions. Instead, any elastic response will be a consequence of residual stress formation and/or material hardening.

The drawback with an FE-based approach is that it requires simulations that are extremely demanding. Some key issues:

- The simulations need to feature a material model that can account for non-linear kinematic hardening to capture the “roll-out” of the rail steel.
- Contact, including plastic deformations, need to be established for two conformal surfaces. This puts extreme demands on the FE-solver.
- Large deformations (including major rigid body displacements) need to be accounted for.
- At least three (and preferably more) rollovers need to be simulated to obtain a stabilised material response. These rollovers need to cover a sufficiently long distance on the railhead.

In [5] simulations for the DB rig are presented. These simulations show that the results are very sensitive to load and contact configuration despite the fact that plastic deformations generally tend to “smear out” small irregularities. The simulations carried out within INNTRACK also demonstrated that the simulations are currently on the limit of what can be achieved. In order to get any results at all a large number of control variables had to be tuned (corresponding to months of trial simulations). Even then, a bug (or lack of accuracy) has prevented a proper analysis of the voestalpine test rig

Still it is likely that as computational power increases, predictions based on FE evaluations of stresses and strains coupled with low-cycle fatigue/ratcheting prediction will be the future.

5.2.4 Conclusions and recommendations

The aim of the studies D4.3.4 [4] and D4.3.5 [5] was to link laboratory testing to field conditions through numerical simulations. The study show $F_{l,surf}$ -based RCF predictions to be a promising approach in this respect. To establish the suitability further, and the expected scatter in predictions, further test cases need to be analysed. For twin-disk tests, this is fairly straightforward. For full-scale test rigs, the situation is much more complicated due to the conformal contact. The following issues that be considered for these cases:

- The evaluation of the contact patch size and normal contact stresses poses difficulties for full-scale test rig conditions. To get realistic results it is needed to know the point of contact and to adopt non-hertzian contact theory as discussed in section 5.1. To facilitate numerical evaluations, the contact geometry can be controlled to limit the conformity in the point of contact so that hertzian theory may be employed. This will however decrease the similarity between test rig and field conditions.
- The need to account for non-hertzian contact conditions currently also limits the possibility of adopting simulations of dynamic wheel–rail interaction. Consequently, parameters such as wheel–rail slip cannot be adopted in an equivalent RCF measure since they cannot be evaluated in a reliable manner. There is work in progress to overcome these difficulties, so the situation is likely to improve.
- A reliable evaluation of the interfacial friction in terms of both maximum coefficient of friction and actual traction coefficient is crucial to obtain reliably RCF predictions. For cases where numerical simulations may not give guidance (as discussed above), direct or indirect measurements of these parameters are the only possibility.
- Due to the complexity of numerical simulations, laboratory conditions that vary periodically (e.g. oscillating lateral loads and/or intermittent water spraying) are not recommended. The reason is that only some few cases in the continuous variation can practically be evaluated. To obtain a full evaluation there will then be a need for interpolations/extrapolations that will decrease the reliability of the predictions.

In addition to $F_{l,surf}$ -based RCF predictions, also FE-based predictions have been studied in INNTRACK. Currently the simulations are too computationally demanding and numerically sensitive to be operational in production environments. However, as computational power increases and modelling techniques improve, it is likely that FE-based techniques will take over as main approach to simulate laboratory tests numerically.

6. Overall assessment of the tests

The WP 4.3 group decided to compare the different test methods qualitatively by giving notes in a table. Additionally the effort needed for doing the tests was estimated by the performers themselves.

The comparison is shown Table 6 where the following rating was used:

- 1, 2 – more or less far from practical requirements or expectations
- 3 – acceptable compromise between practical demands and testing capabilities
- 4, 5 – good or excellent agreement to practical requirements or expectations

Table 6: Qualitative comparison of the rail test methods

	<u>Not e</u>	<u>UoN / SUROS machine</u>		<u>VAS RSP test rig</u>		<u>DB test rigs</u>
Test specimen						
Rail test sample	3	cylindrical disk; Ø47 mm	5	rail segment, 1,5 m	2	bended or rolled rail material
Rail material	5	any desired (even prototypes)	4	arbitrary	2	specific
Wheel counterpart	3	cylindrical disk; Ø47 mm	4	single wheel, original sized	5	wheelset, original sized
wheel material	5	any desired (even prototypes)	5	arbitrary	5	arbitrary
Contact conditions						
wheel and rail profiles	3	line contact	5	S1002/UIC 60	5	S1002/UIC 60
Nominal contact Forces	4	~7,14 kN (downscaled)	4	200 kN vertical 40 kN lateral (200% magnified)	5	2x80 kN vertical ~ 5 kN lateral (real sized)
Lateral forces	2	none	5	< 40 kN	3	<10 kN
slip	4	1 % (too large for non-driven wheels)	4	none (too low for driven wheels or braking)	4	none (too low for driven wheels or braking)
lubrication	3	water	3	(water)	4	water spray
angle of attack	3	none	3	none	5	< 8 mrad
Quality of test results						
stability of test results	4	good	4	good	1	mechanical failure
correlation to simulation	4	good	4	good	3	medium
comparable material deformation	4	good	4	good	3	medium
comparability to field conditions	3	medium	4	good	-	not evaluated

In Table 7, an estimate of the effort for the different test methods is given. It is based on the time required for preparing and performing the test and data collection. It should be noted that preparing the rail specimen and the contacting wheel needs additional efforts for the tests.

Nevertheless, twin disk testing seems to be the method with the lowest overall cost while full-scale roller rig tests need expensive preparing of rail profiles.

Table 7: Rough estimate of efforts needed for one test

	samples & material needed	estimated time for test preparation and follow-up (*)	estimated duration of the test (**)	estimated time for measurement and data collection (***)
Twin disk, SUROS	special test sample, Ø47 mm	one hour	one hour	one hour
Linear test rig VAS RSP	rail segment, 1500 mm single wheel with new S1002 profile	3 man-day	5 days	2 man-days
Roller test rigs DB, C and A	2 rings of rail material newly profiled wheelset with bearing, new 1002 profiles	3 man-days	1 week	2 man-days

* includes all objects needed for performing the test, i.e. the samples to be tested and their counterpart.

** includes the man-time needed for establishing one test configuration at the rig

*** includes the man-time needed for doing measurements, storing and evaluating data etc. This does not include the time needed for an overall evaluation of all results after a test campaign.

7. Conclusion

It could be shown that twin disk tests represent a good way of testing rail materials under closely controlled conditions. In transferring the laboratory results to field conditions one has to consider that the twin disk configuration represents extreme wear because of permanent slip under dry and clean high friction conditions and because the influence of the profile shapes cannot be taken into account. The related tests under partial wet conditions appeared to have not the required stability.

The full-scale tests of VAS and DB demonstrated that real contact conditions could be established even in the laboratory. Subsequent numerical calculations have shown that the real contact point and rail inclination deviate from the planned position because of deflections within the test rigs. This has to be taken into account when test results are to be transferred into field conditions or when numerical multi-body calculations are performed on this basis.

At the VAS full-scale rail-wheel test it could be demonstrated that for pearlitic rail steels an increased wear resistance correlates with an increased RCF resistance. Moreover, the VAS test rig clearly shows the same trends as seen in track: heat-treated rail grades (R350HT, 400BHN grade) show an increased Wear and RCF resistance compared to the standard not heat-treated rail grade R260.

At the DB full-scale roller rig, the required test conditions could not be established. Although parts of a real railhead were specifically bended for a test environment and a new, special fixing for mounting the rails was used, the construction was not sufficiently stable. Moreover, the subsequent metallographical analysis the railhead showed that the depth of damage layer was below expected parameters known from the field.

All test results were reviewed afterwards by metallographic analysis as well as by numerical contact analysis. It could be shown that the results are mainly comparable to findings from the field. Predictions on the RCF initiation could be established based on the tests.

8. References

References to be found in INNTRACK KMS

- [1] INT D4.3.1: Testing Matrix Definition. Responsible: DB, author: Ullrich, D, published Aug. 2007.
- [2] INT D4.3.2: Characterisation of microstructure. Responsible: Corus, author: Jaiswal, J, published Oct. 2007.
- [3] INT D4.3.3: Results of first tests. Responsible: DB (with contributions of UoN and VAS), author: Ullrich, D, published May 2008.
- [4] INT D4.3.4: Contact stress and wear. Responsible: TUD, author: Li, Z., published Oct. 2008.
- [5] INT D4.3.5: Simulation of material deformation an RCF, Responsible: Chalmers, author: Kabo, E/ Ekberg A., published July. 2009.
- [6] INT D4.3.6: Characterisation of microstructure. Responsible: Corus, due: July 2009.
- [7] INT-SP43-30-090815-D5-SUROS-TWIN-DISC-TEST-RESULTS.DOC, University of Newcastle upon Tyne, U.K., authors: Franklin, FJ/Fletcher, DI/Vasic, G, published Aug. 2009
- [8] INT-SP43-05-090806-F1-RSP_Tests_R260_R350HT_400BHN_dry: Results of VAS RSP-Tests, VAS, author: Stock, R, published Aug. 2009.
- [9] Johnson K L, The strength of surfaces in rolling contact, IMechE, Mechanical Engineering Science, vol 203, pp 151-163, 1989
- [10] Ekberg A, Kabo E & Andersson H, An engineering model for rolling contact fatigue, Fatigue & Fracture of Engineering Materials & Structures, vol 25, pp 899-909, 2002

9. Appendix 1: Measurement of RCF under laboratory testing conditions

(Final version contributed by Corus Rail Technologies, author Carroll, R)

General

To allow accurate and consistent measurement of rolling contact fatigue (RCF) cracks during laboratory testing, a methodology is required which can be followed by all partners. This document discussed within WP4.3 is based on Corus and Network Rail's experience of measurement of RCF cracks during track trials.

Before any sectioning is carried out a close inspection of samples, with photographs taken (preferably with a ruler) should be carried out. A rail profile should be taken using a Miniprof or similar if appropriate. The surface of the sample should be inspected as specified in following section.

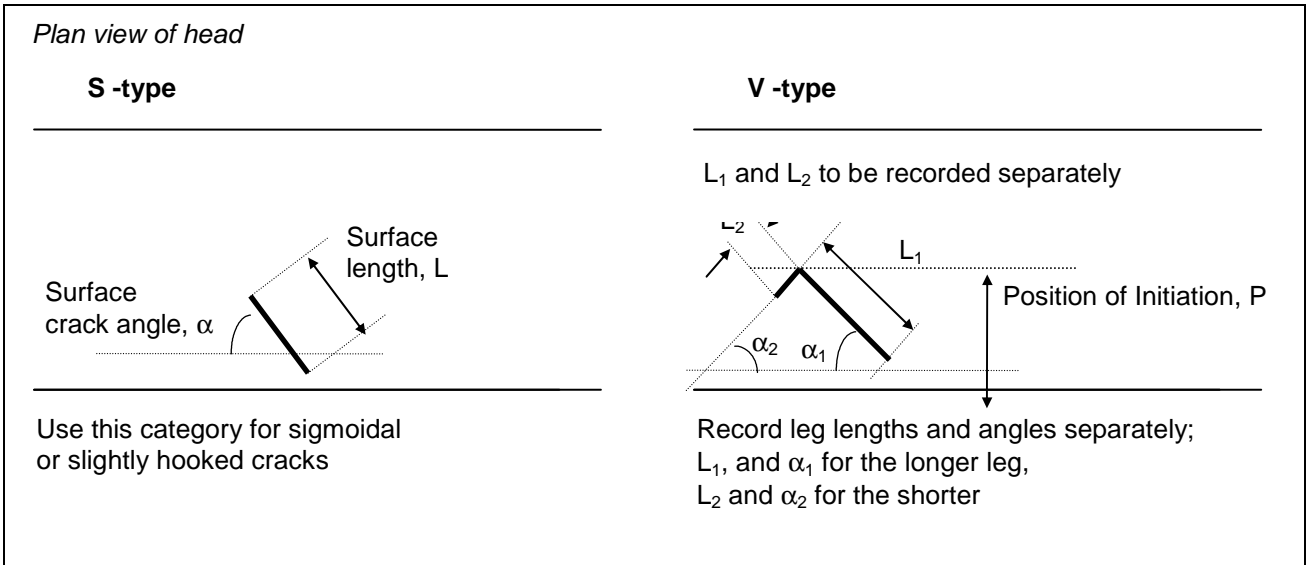
Surface Cracks

The following information needs to be recorded for all test samples. Cracks may need to be highlighted using magnetic particle or liquid penetrant inspection to aid identification.

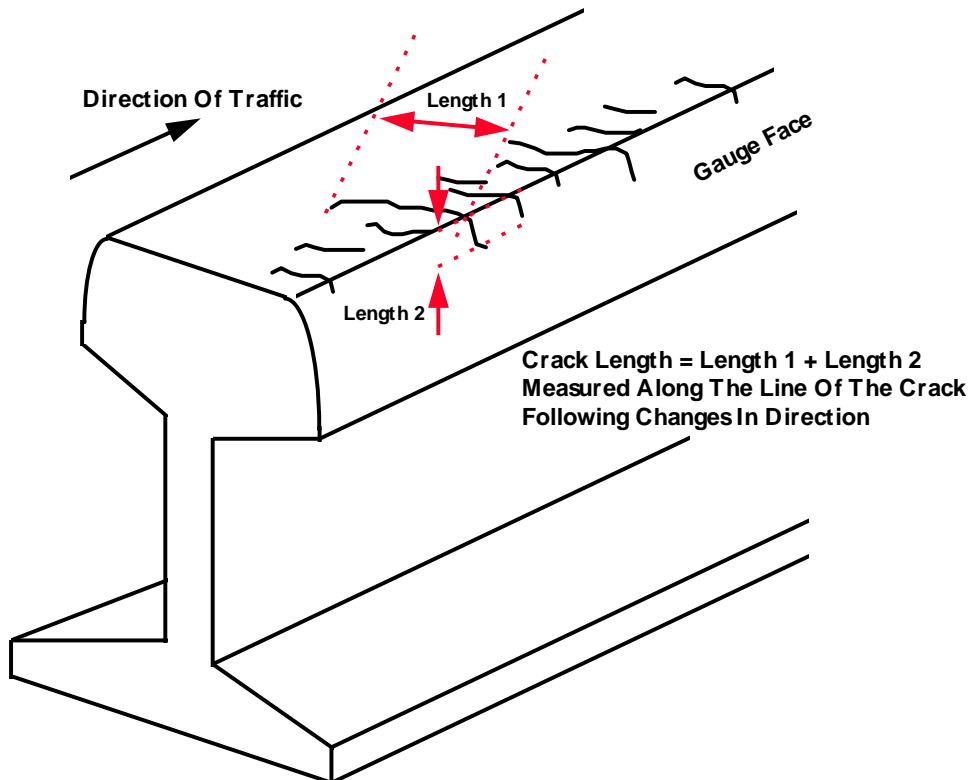
- A photograph of the surface of the sample should be taken, preferably with a ruler included against the surface of the sample.
- The lengths and angles of approximately six of the longest cracks should be recorded. If cracking extends down the gauge face, this length should also be included in the measurement of total crack length. For details, see Table 1 and the following sketches.
- Position of initiation of cracks
- Density of cracking, i.e. reciprocal of longitudinal spacing of the cracks.

Symbol	Description
L, L _n	Surface crack length,
α , α_n	Surface crack angle measured parallel to running direction
P	Position of Initiation, distance from gauge corner to furthest tip of crack.
D	Subsurface depth of crack perpendicular to surface
K, K _n	Subsurface crack length, distance along the crack
ϕ , ϕ_n	Angle of subsurface crack from surface

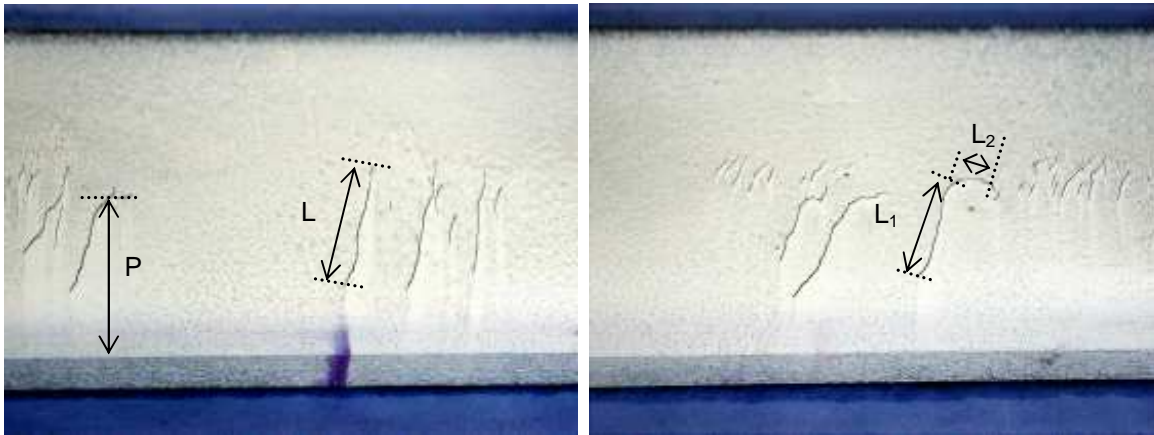
At least two different types of RCF cracks have been identified these are shown schematically in the diagrams below with a definition of the measurements required of the surface crack features for each.



Where cracks propagate below the gauge corner then the crack length reported should be the total along the surface and on the gauge face, see below.

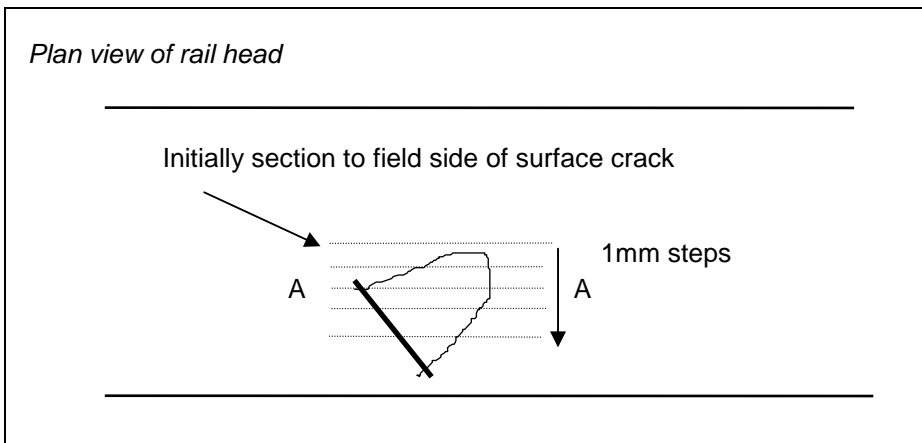


Examples of RCF cracks with measurements

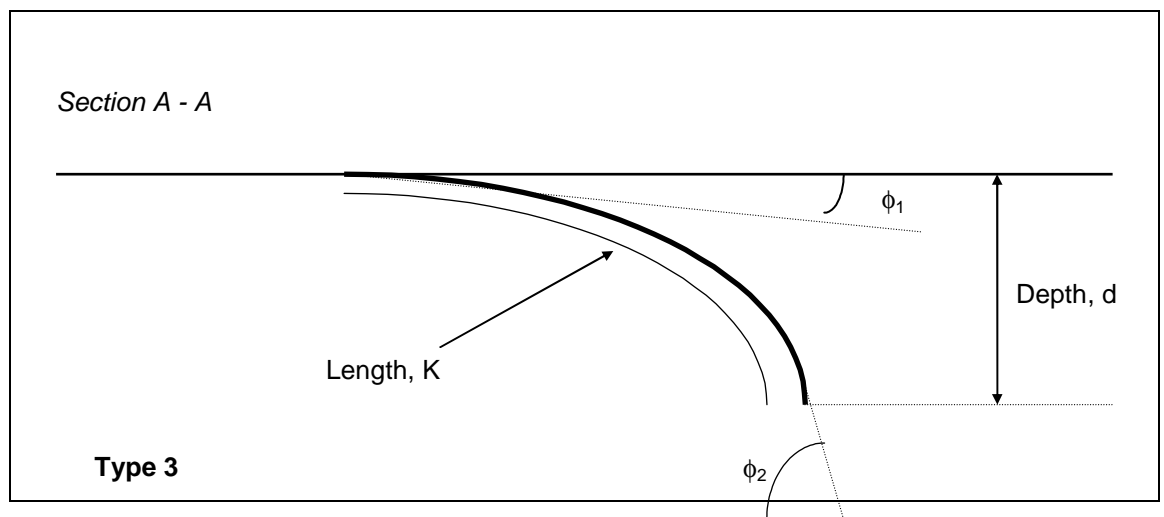
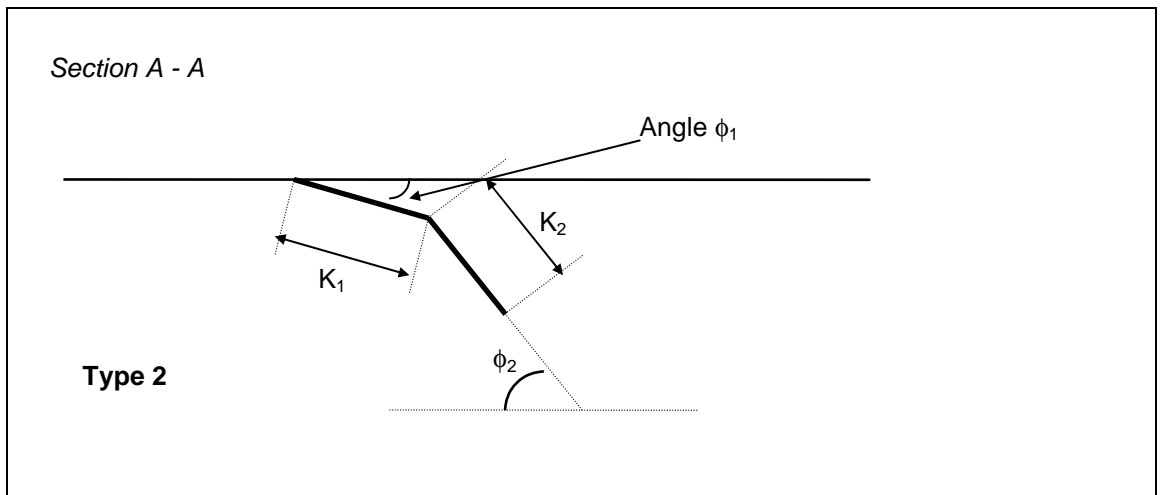
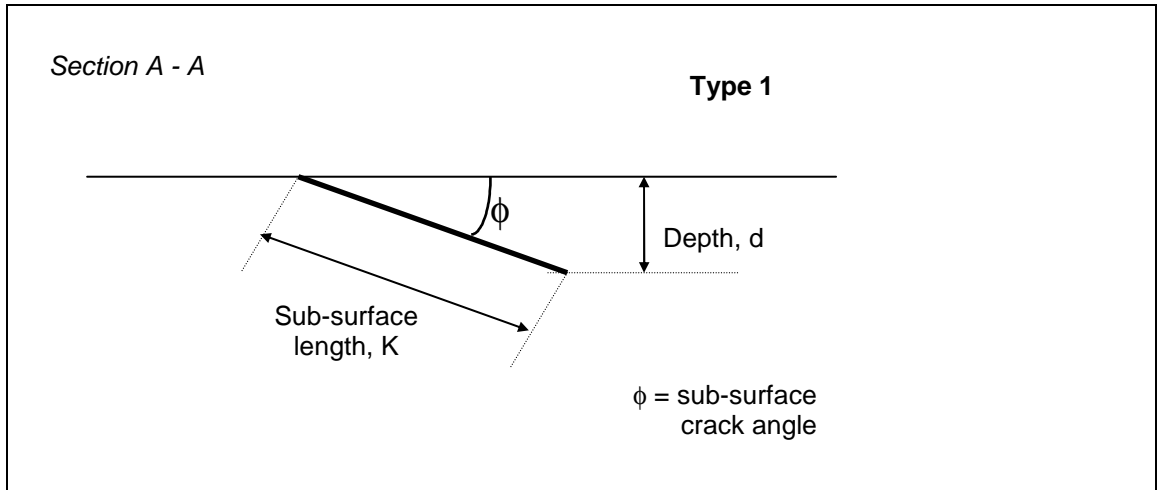


Subsurface Cracks

To study the propagation of cracks below the surface the samples should be sectioned longitudinally, initially this should be on the field side of the surface crack. The sample should then be milled or ground in 1mm steps to reveal the location of the deepest crack.



Cracks can propagate in several ways below the surface. The required measurements depend on the morphology. They are shown below.



Samples should also be sectioned for metallurgical analysis. The samples should be prepared in the standard metallographic way as e.g.: mounted in Bakelite (conducting if examination in SEM is required), surface grinding carried out to ensure parallel surfaces etc.

The sample should be ground on SiC grinding papers. Grinding should be carried out using papers with increasingly smaller grit size e.g. starting with 120 grit and working progressively through 240, 400, 800, and 1200. The sample should be cleaned with running water between papers to remove any particles before proceeding on to the next paper. Care should be taken to reduce bevelling of edges of sample.

Once samples have been ground on finest paper samples should be cleaned using cotton wool, detergent (Teepol) solution and water before rinsing in alcohol and drying. Samples should be polished using diamond paste of $6\mu\text{m}$ and $1\mu\text{m}$ on a rotating pad. Samples should be cleaned using the same process between pads and after polishing.

The samples should be etched using 1% or 2% Nital (nitric acid diluted in methanol) for between 2 and 5 seconds and washed with copious amounts of water, dried and rinsed in alcohol.

Samples should be stored in desiccators to preserve the etch. After extended storage, samples should be re-polished and etched.

Observation in optical microscope and photographs of deformed microstructure below surface should be carried out. Preferably, scale bars should be embedded into micrographs or alternatively magnification recorded.

To characterise deformation of rail material below surface then microhardness traverses using a Vickers microhardness indenter (100 or 200g) should be carried out until bulk hardness values are reached at spacings of not less than $5\times$ width of indent.